研究報告２４

Terahertz Emission from GaAs and InAs Thin Films Grown on Si Substrates in the Transmission-geometry Optical Excitation

Elmer Estacio[1], Christopher T. Que[1], Kohji Yamamoto[1], Masahiko Tani[1], Satoru Takatori[2], Minh Hong Pham[2], Takashi Yoshioka[2], Marilou Cadatal-Raduban[2], Nobuhiko Sarukura[2], and Masanori Hangyo[2], Tadataka Edamura[3], Makoto Nakajima[4], John Vincent Misa[5], Rafael Jaculbia[5], Armando Somintac[5], and Arnel Salvador[5]

[1]*Research Center for Development of Far-Infrared Region, University of Fukui Fukui 910-8507, Japan*
[2]*Institute of Laser Engineering, Osaka University, 2-6 Yamadaoka, Suita, Osaka 565-0871, Japan*
[3]*Central Research Laboratory, Hamamatsu Photonics K.K., Hamamatsu 434-8601, Japan*
[4]*Institute for Solid State Physics, University of Tokyo, Kashiwa, Chiba 277-8581, Japan*
[5]*National Institute of Physics, University of the Philippines, Diliman Quezon City 1101, Philippines*

Abstract

We report on the generation of intense terahertz (THz) pulses from femtosecond laser-illuminated InAs and GaAs thin films grown on Si substrates. The InAs/Si and GaAs/Si films' THz emission were shown to be possible in both reflection and transmission-geometry excitation cases. The InAs/Si film exhibited weaker emission but is expected to be more feasible as a spectroscopic THz source due to the absence of complex spectral features in its emission spectrum. The GaAs/Si emission is characterized by Fabry-Perot oscillations but is 90% that of p-InAs bulk crystal emission intensity in the reflection geometry. Excitation fluence measurements showed that the InAs/Si film saturates easily due to the laser's shallow penetration depth in InAs. In a related work, the THz emission characteristics of the GaAs/Si films under an applied magnetic field were also studied and a peculiar polarity dependence of the enhancement characteristics was observed.

1. Introduction

Terahertz (THz) ultrashort pulses from surge current and optical rectification in femtosecond laser-irradiated semiconductor surfaces have been extensively studied in pursuit of easy-to-use and intense pulsed THz emitters [1-4]. Bulk p-type InAs has long been well regarded as the most intense semiconductor surface emitter [1], while GaAs is widely employed as THz photoconductive antennae and surface emitter devices [3]. In the context of effective mass and carrier mobility, GaAs has been considered inferior to bulk InAs [3]. However, GaAs-based device fabrication protocols are well established and they should still be viable for applications in future THz optoelectronics devices design. Additionally, Si is an integral component in THz optics; in which its property of being transparent in this frequency region has made it a standard material for substrate lenses [5-7]. In this regard, an effort to integrate two of the most widely used semiconductor THz emitters into the highly-established Si technology can be crucial in integrating THz science in the mainstream semiconductor industry. Previously, there have been significant works in growing high-quality GaAs films on Si and even InAs films on Si, which were intended for applications in high-speed optoelectronics [8-11]. Quite recently, THz generation from InAs/Si thin films in the transmission excitation geometry was reported [12]. In this current work, we report on the intense THz emission from femtosecond laser-irradiated GaAs and InAs thin films grown on Si substrates (GaAs/Si and InAs/Si), grown by molecular beam epitaxy (MBE). Results show that for these samples, THz emission is possible for both reflection and transmission excitation geometries; which offer further ease-of-alignment and can expand the practical applications of these THz emitters. As an additional study, the magnetic field-induced THz emission enhancement characteristics for GaAs films grown on Si(100) and Si(111) substrates were investigated and the results exhibit peculiar polarity dependence properties.

2. Experiment

Shown in Table 1 is the summary of the MBE-growth specifications of the two samples that were studied. The undoped InAs thin films were grown on aluminum antimonide- (AlSb) buffered (100) Si substrates. The 350 μm-thick, high-resistivity (>1 kΩ.cm) Si substrates were chemically and thermally treated inside the growth chamber, prior to growth. The extremely large lattice mismatch between InAs and Si, necessitates the growth of an AlSb buffer layer[13]. This is lattice-matched to InAs and primarily smoothens out the growth surface prior to the InAs film deposition.

Sample	Si Substrate Doping type	Buffer layer (thickness) (nm)	Grown Layer (thickness)
InAs/Si	350 μm -thick (100) high-resistivity Si	AlSb (100 nm)	InAs thin film (520 nm)
GaAs/Si	310 μm-thick (100) n-doped Si	None	n-doped GaAs (500 nm) followed by undoped GaAs (500 nm)

Table 1. A summary of the MBE-growth specifications of the InAs/Si and GaAs/Si films.

The AlSb buffer layer was grown at 510 ^{o}C while the InAs layer was grown at 410 ^{o}C with a growth rate of 0.3 μm/h. In this study, the InAs layer had a thickness of 520 nm. The AlSb buffer layer thickness was 100 nm, while reflection high-energy electron diffraction patterns showed that the grown InAs films were single crystals. The GaAs/Si samples were grown on 500 μm-thick, (100) n-type Si wafers (1-10 Ω.cm resistivity) acquired from Hefei Keijing Materials Tech. Co. The substrate was chemically etched prior to loading into the MBE and heated to 740 ^{o}C for oxide removal prior to growth at 680 ^{o}C. A 500 nm n-type GaAs was initially grown and this was subsequently followed by a 500 nm-thick undoped GaAs layer. The substrate was then mechanically lapped to reduce the Si substrate thickness to 310 μm. Both MBE-grown thin film samples have the same crystal orientation as their respective (100)-oriented Si substrates. Firstly, the THz emission from the InAs/Si and GaAs/Si samples were compared with bulk p-type InAs emission in the reflection excitation geometry as shown in Fig.1(a). The excitation came from a mode-locked Ti:Sapphire laser delivering 100 fs pulses centered at 800 nm, at a repetition rate of 80 MHz. In this excitation geometry, the laser was made incident on the samples at a 45^{0} with respect to the surface. The THz emission was collected in the specular reflection direction while a cryogenic Si bolometer operating at 4.2K coupled to an FTIR spectrometer was used to record the emission spectra. The terahertz emissions in the transmission excitation geometry were measured using THz time-domain spectroscopy (TDS) as shown in Fig. 1(b). In this case, the fs-laser was used both as the excitation source as well as an optical gate for a photoconductive dipole-type antenna with low-temperature-grown GaAs that was employed as the detector. In this excitation geometry, the p-polarized pump beam was made incident at the Brewster angle (about 70 degrees for the InAs/Si and about 65 degrees for the GaAs/Si) of the samples and the THz radiation transmitted through the Si substrate was focused by a pair of parabolic mirrors on the photoconductive antenna and the photoconductive signal was detected with a lock-in amplifier with pump beam modulation by an optical chopper set at a frequency of 2 kHZ. Moreover, the excitation fluence dependence of the thin films' THz emission was also studied.

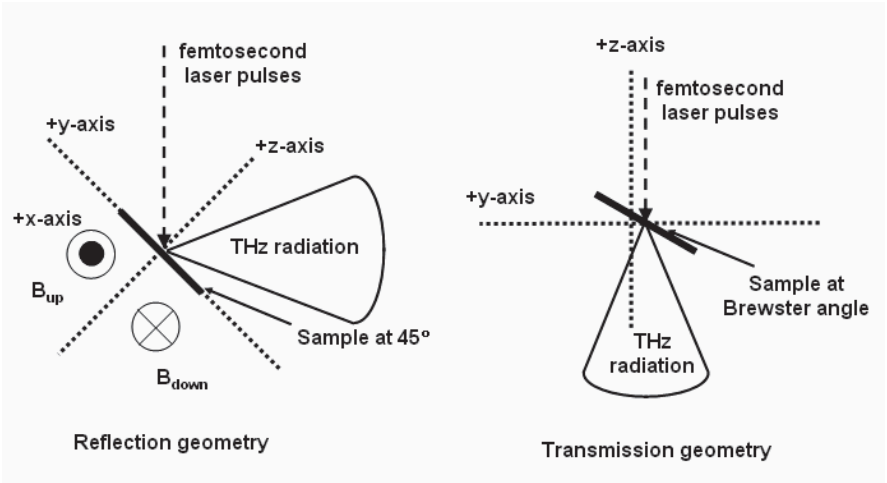

Fig. 1. The schematic diagram of the experimental setup showing the two types of optical excitation geometries that were employed. The coordinate axis corresponds to the laboratory frame. The applied magnetic field polarity is shown in (a) and will be discussed more thoroughly later in the text.

3. Results and Discussion

Figure 2 shows the THz emission spectra in the reflection excitation geometry for the InAs/Si and GaAs/Si samples as compared with (100) p-InAs and semi-insulating (SI) GaAs wafers. The p-InAs wafer was determined to have a carrier concentration of 7.1×10^{16} cm^{-3} and hole mobility of 150 $cm^2/(V.s)$ according to previous Van der Pauw-Hall measurements. The optical alignment and excitation conditions for all the THz measurements were maintained the same. Results show that the p-InAs wafer exhibited the most intense THz emission while the SI GaAs sample showed the weakest. The p-InAs emission is more intense than that of the bulk GaAs by about 2 orders of magnitude in power while the InAs/Si sample's emission power is about 1 order of magnitude stronger than bulk GaAs. The GaAs/Si emission power was observed to be close to the p-InAs crystal. The measured readouts of the broadband THz emission verified that the GaAs/Si emission power is ~90% that of the p-InAs wafer. Moreover, the presence of oscillatory features superposed with the water vapor THz absorption lines in the GaAs/Si and InAs/Si, which are attributed to Fabry-Perot modes in the Si substrates, suggest that the thin film samples are not totally opaque to THz radiation; similar to GaAs.

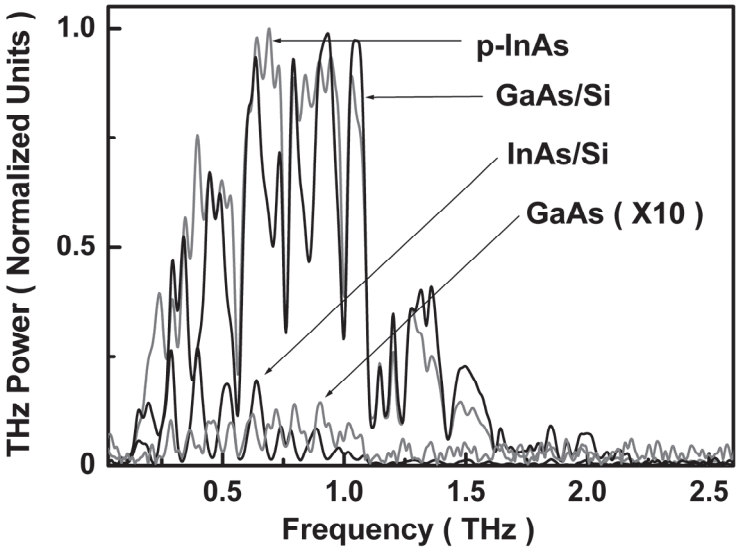

Fig. 2. The THz emission spectra in the reflection excitation geometry for the InAs/Si and GaAs/Si samples, in comparison with p-InAs bulk crystal and GaAs wafers. The InAs/Si emission is roughly 1 order of magnitude stronger than bulk GaAs while the GaAs/Si emission was observed to be almost equal to the p-InAs crystal.

In order to confirm that the MBE-grown layers are not opaque in the THz region, the InAs/Si and the GaAs/Si samples' THz emission were measured in the transmission excitation geometry. Figure 3 shows the TDS plots and the associated amplitude spectra for the thin film samples that were investigated. Three excitation fluence conditions were taken for both samples and no obvious changes in the TDS line shapes were seen except for the expected increase in THz field amplitudes as the excitation fluence was increased. The GaAs/Si TDS amplitude is higher than the InAs/Si sample by a factor of 4 in the transmission geometry. Thus, it can be inferred that the GaAs/Si sample's THz emission power is ~16 times higher than the InAs/Si film emission. Relative to the results in Fig. 2, the GaAs/Si film appears to be even more efficient as a THz emitter in the transmission excitation geometry case. These results imply that even though free-carrier absorption reduces the THz transmission in n-type Si, intense emission was still observed in this excitation scheme. Moreover, the GaAs/Si signal in Fig. 3(a) is composed of multiple transient signals after the initial pulse and is due to multiple reflections from the front and back surfaces of the GaAs/Si sample. The InAs/Si TDS signal in Fig. 3(b), however, is mainly composed of only an almost single-cycle pulse having a slightly broader pulse-width. These differences are even more evident in the insets showing the amplitude spectra taken from the Fourier transform of the TDS data. The InAs/Si THz emission is shifted towards lower frequencies with respect to the GaAs/Si.

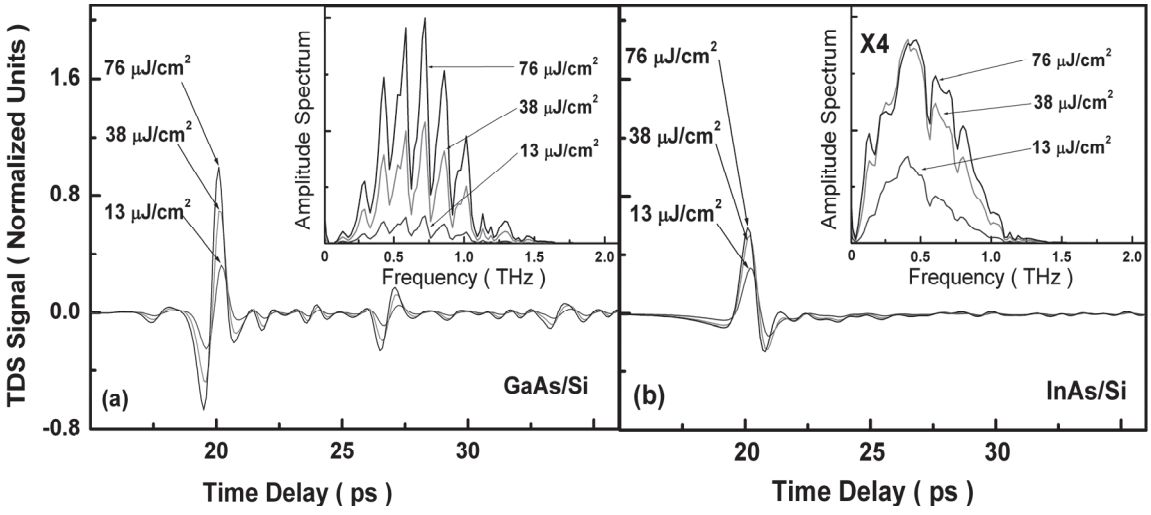

Fig. 3. The TDS plots and the associated amplitude spectra for the InAs/Si and GaAs/Si thin films.

At present, the exact origin of this observation cannot be explained but a plausible explanation lies in the samples' different in the dominant THz radiation mechanism. The drift-related emission in GaAs occurs almost instantaneously as the photocarriers are created and are accelerated by the electric field. The photo-Dember emission in InAs, however, results from the net diffusion current due to the different velocities of the electrons and the holes; and should occur at a later time. This manifests as a comparatively slow-varying TDS slope resulting in a lower-frequency spectral peak. It can be

observed that the lineshape of the GaAs/Si amplitude spectrum is characterized by Fabry-Perot modes while that of the InAs/Si sample possesses less spectral features. Although the GaAs film is thicker than the InAs film, GaAs is more transparent to THz radiation [14]. Thus, in the transmission excitation geometry the GaAs/Si sample should act as a more efficient Fabry-Perot cavity compared with the InAs/Si. Owing to this, the InAs/Si sample appears to be more feasible as an optical source for THz spectroscopy applications due to its emission's well-behaved spectral shape. Moreover, the expected emission enhancement by the application of a modest-level magnetic field in InAs makes the InAs/Si even more viable.

Excitation fluence dependence studies were also performed on the samples' THz emission in the transmission geometry and the results are shown in Fig. 4. The square and circle symbols are the experimental data for the pump fluence dependence of the THz emission peak amplitudes for InAs/Si and GaAs/Si, respectively. The lines are least squares fits of the expression, $A/(1+F_{sat}/F)$, where F is the fluence, F_{sat} is the saturation fluence, and A is just an amplitude scaling factor [3]. The best fit lines revealed saturation fluence values of ~15 μJ/cm2 and ~58 μJ/cm2 for InAs/Si and GaAs/Si, respectively. The factor of 4 difference of the saturation fluence is a very interesting result. It is in contrast with the previously known THz emission properties of bulk InAs and GaAs. Bulk InAs has been previously established to be a more efficient THz emitter compared with GaAs and that the former emits via photo-Dember effect while the latter emits via field-driven photocarrier drift [2,3].

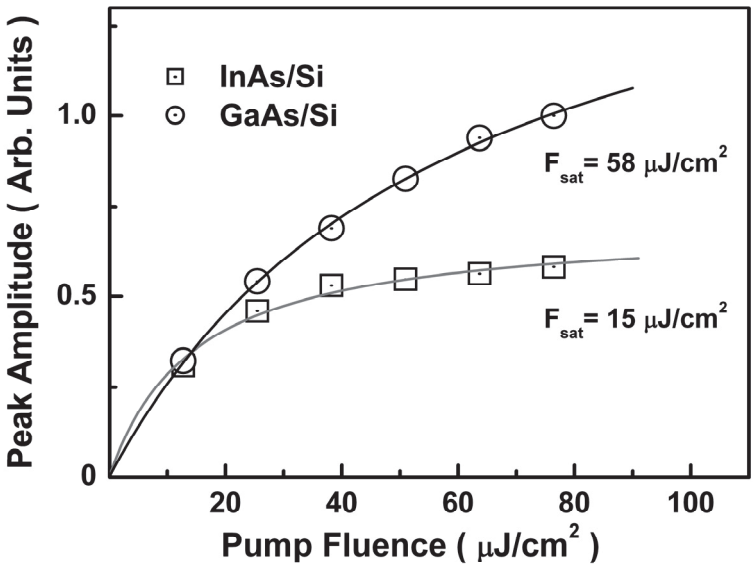

Fig. 4. The excitation fluence dependence of the samples' THz emission in the transmission geometry. The symbols are the experimental data while the lines are least squares fits to the expression, A/(1+Fsat/F), where Fsat is a saturation fluence fitting parameter. The best fit lines revealed saturation fluence values of ~15 μJ/cm2 and ~58 μJ/cm2 for the InAs/Si and GaAs/Si, respectively.

These results are explained in terms of the differences in the THz radiation and saturation mechanisms of these two samples as well as differences in the excitation laser's penetration depth. The penetration depth of 800 nm-wavelength light in InAs is only about 140 nm while it is ~1 μm for GaAs [3,15]. For the InAs/Si sample, its saturation fluence is limited by the photocarrier density and not by electric field effects. Due to the laser's shallow penetration depth, carrier density buildup occurs easily. Thus, carrier accumulation possibly causing carrier-carrier scattering resulted into the lower saturation fluence in the InAs/Si sample [3]. In contrast, the field-driven photocarrier drift THz radiation mechanism and the ~1 um laser penetration depth in the GaAs/Si sample, elicited higher saturation. Primarily, the deeper laser penetration resulted into a lower photocarrier density; thereby setting back the adverse effects of electric field screening which leads to saturation.

The overall advantage in the THz emission intensity of the GaAs/Si film over InAs/Si is explained by its structure. Terahertz emission in GaAs is attributed to the depletion field drift of the carriers as they are swept across a high electric field region and in the 1 μm-thick GaAs film, there are three of these high electric field regions in concern. These are the GaAs surface, the undoped GaAs/n-type GaAs interface, and the n-type GaAs/n-Si interface. Firstly, the photocarrier carrier drift due to the GaAs surface field, contributes to the THz emission. As for the undoped GaAs/n-type GaAs interface, a previous work demonstrated the order-of-magnitude enhancement (as compared to SI-GaAs) in the THz generation intensity for undoped-GaAs/ n-GaAs layers, owing to the design of the depletion layer at the interface [16]. The same principle can be used to account for the origin of some of the enhancement in the THz emission from the GaAs/Si film. Accurate depletion layer comparisons cannot be made but a 1 order of magnitude enhancement may be estimated. As such, the ~2 orders of magnitude increase in the GaAs-related THz emission of the GaAs/Si sample is presently attributed to the additional contribution of the depletion field at the n-GaAs/n-Si interface. This interface is expected to be under high electric field due to the difference in the band structures of n-GaAs and n-Si. Moreover, there is a 4% lattice mismatch between these two materials [9]. As such, a piezoelectric strain field is speculated to arise at this interface region which may aid in the more efficient sweeping of the photogenerated carriers to generate drift-related THz emission.

As an additional study, a different set of GaAs films were simultaneously grown on (100) and (111)-oriented n-Si substrates. The THz emission spectra were then measured in the reflection geometry excitation to compare the relative intensities and frequency bandwidths of the detected THz emission. Figure 5 shows the THz emission spectra of SI bulk GaAs, GaAs/n-Si(100) and GaAs/n-Si(111) for 3 cases (No B, B_{UP}, and B_{DOWN} where the B field directions are illustrated in Fig. 1). The data are normalized with respect to GaAs/n-Si(100) in the B_{UP} case. The bulk GaAs emission in Fig. 3(a) has a narrower bandwidth compared with either GaAs/n-Si samples in Figs. 3(b) or (c) whose emissions extend to 1.5 THz. The THz emission from GaAs/n-Si(100) is observed to be higher than the GaAs/n-Si(111) and this may be due to a better GaAs film quality for the (100)-grown layer. It has been previously reported that that, Si(100) substrates induce less biaxial strain on the GaAs layer [17]. Oscillatory features can be easily seen in the bulk GaAs emission spectrum; which is ascribed to

Fabry-Perot modes generated from the front and back surfaces of the bulk GaAs wafer. The mode spacing agrees well with the GaAs wafer's nominal thickness of ~600 μm. For the MBE-grown layers, the modes are not as evident as in the bulk GaAs case. Moreover, the magnetic field polarity dependence of the THz emission presents peculiar results. In general, an externally applied magnetic field (regardless of polarity) enhances the THz emission where a preferred field polarity yields higher enhancement; as in the case of the bulk GaAs data. In the GaAs/Si samples' cases, however, the B_{UP} case strengthened the THz emission, but in the B_{DOWN} case the emission was drastically reduced. This may be explained by the dependence of the magnetic field-enhanced THz emission intensity on the interface roughness and has been reported, previously[18]. In this situation, a photogenerated carrier under the influence of the Lorentz force interacts more strongly with the interface layer in the B_{DOWN} case than in the B_{UP} case; making it more prone to scattering. This results into the reduction of the magnetic field enhancement. However, in this current work, the THz emission was drastically diminished to levels even lower than in the NO B case. These magnetic field dependence characteristics of the THz emission have not been observed, previously. This suggests that the GaAs/Si interface is not only strained but is also very rough at the same time.

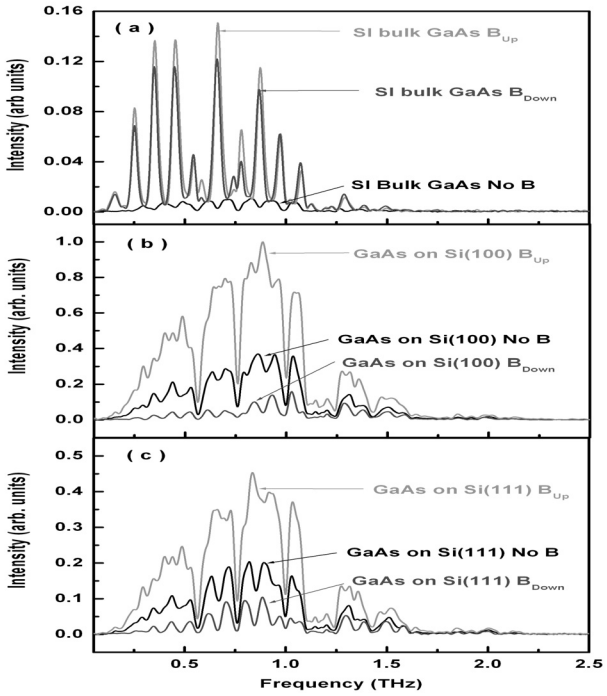

Fig. 5. The THz emission spectra for No B, BUP, and BDOWN cases from (a) SI bulk GaAs wafer, (b) GaAs on n-Si(100), and (c) GaAs on n-Si(111). Additionally, the THz emission enhancement from the GaAs/Si samples are very sensitive to the polarity of the applied magnetic field while the bulk GaAs wafer exhibited radiation enhancement regardless of the field polarity.

References

[1] N. Sarukura, H. Ohtake, S. Izumida, and Z. Liu, J. Appl. Phys. **84**, 654 (1998)

[2] M. B. Johnston, D. M. Whitaker, A. Corchia, A. G. Davies, and E. H. Linfield, Phys. Rev. B **65**, 165301 (2002).

[3] P. Gu and M. Tani, in Terahertz Optoelectronics, Topics in Applied Physics Vol. 97, edited by K. Sakai (Springer, Berlin, 2005), pp. 24,63–76, 15-153.

[4] M. Reid and R. Fedosejevs, Appl. Opt. **44**, 149 (2005).

[5] P. Uhd Jepsen and S. R. Keiding, Opt. Lett. **20**, 807 (1995)

[6] D. Grischkowsky, S. Keiding, M. van Exter, and Ch. Fattinger, J. Opt. Soc. Am. B. **7**, 2006 (1990)

[7] Y.-S. Chung, C. Cheon, J.-H. Son, and S.-Y. Hahn, IEEE Trans. Mag. **36**, 951 (2000).

[8] R Kromer, Journ. Cryst. Growth **81**, 193 (1987).

[9] W. Stolz, F. E. G. Guimaraes, and K. Ploog, J. Appl. Phys, **63**, 492 (1988)

[10] S. Kalem, J. Chyi, C.W. Litton, H. Morkoc, S. C. Kan, and A. Yariv, Appl. Phys. Lett. **53**, 562 (1988).

[11] D. J. Oostra, R.V. Smilgys, and S.R. Leone, Appl. Phys. Lett. **55**, 1333 (1989)

[12] C.T. Que, T. Edamura , M. Nakajima ,M. Tani , and M. Hangyo, Jap. Journ. Appl. Phys. **48**, 010211 (2009)

[13] G. Balakrishnan, S. Huang, L. R. Dawson, Y.-C. Xin, P. Conlin, and D. L. Huffaker, Appl. Phys. Lett. **86**, 034105 (2005)

[14] C. Weiss, R. Wallenstein, and R. Beigang, Appl. Phys. Lett. 77, 4160 (2000)

[15] D.-F. Liu and D. Xu, Appl. **46**, Opt. 10, 789 (2007).

[16] H.. Takeuchi, J. Yanagisawa, T. Hasegawa, and M. Nakayama, Appl. Phys. Lett. **93**, 081916 (2008.)

[17] Z. Sobiesierski, D. A. Woolf, D. I. Westwood, R.H Williams, Appl. Phys. Lett. 58, 628-630 (1991)

[18] E. Estacio, N. Sarukura, C. Ponseca, Jr., A. Somintac, M. Bailon-Somintac, A. Garcia, A. Salvador, J. Appl. Phys. 104, 073506 (2008)